ELSEVIER

Physica B 244 (1998) 27–32

PHYSICA B

Far-infrared study of superconducting $Tl_2Ba_2CaCu_2O_8$

Axel M. Zibold[a,*], David B. Tanner[a], Helmuth Berger[b]

[a] *Department of Physics, University of Florida, Gainesville, FL 32611, USA*
[b] *Département de Physique, EPFL, CH 1015 Lausanne, Switzerland*

Abstract

We report the *ab*-plane optical properties of a $Tl_2Ba_2CaCu_2O_8$ single crystal with $T_c = 110$ K. Measurements were made over 130–30 000 cm^{-1} at room temperature and over 130 and 3000 cm^{-1} at temperatures between 10 and 300 K. The real part of the optical conductivity, determined by Kramers–Kronig analysis, has a metallic behavior above T_c in the far infrared, but non-Drude behavior at higher frequencies. Below T_c, the far-infrared spectral weight is substantially reduced, although there is no superconducting gap feature in the spectrum. A generalized Drude analysis of the conductivity yields a frequency-dependent scattering rate which develops a threshold around 1000 cm^{-1} in the superconducting state. No strong indication of this threshold can be seen above T_c. An alternative two-component analysis also fits the optical data. We found that about 20% of the total doping-induced spectral weight and about 90% of the free-carrier spectral weight contributes to the superfluid condensate. The London penetration depth is about 1700 Å. We conclude that our sample is in the clean limit and close to optimal doping.

Keywords: Superconductivity; High-temperature superconductors; Optical properties; $Tl_2Ba_2CaCu_2O_8$; Far-infrared spectroscopy

1. Introduction

Optical spectroscopy is a powerful tool for the study of charge properties in high-temperature superconductors. These materials have three distinct doping regimes: underdoped, optimally doped, and overdoped. These regimes are typically specified in terms of the behavior of T_c, but there is distinctive behavior in transport and other properties as well [1]. Over this entire doping regime a non-Drude behavior is found in the optical properties. Two different approaches are used to describe this unconventional spectrum [2, 3]. The two-component model assumes two types of charge carriers in the conducting CuO_2 planes: a Drude band, which has a constant (but temperature-dependent) scattering rate, and a (temperature-independent) midinfrared absorption band. In contrast, one-component models are used to represent a strongly interacting electron system with a frequency-dependent scattering rate. Recently, this one-component approach has been used to analyze optical measurements on different single-layer and bilayer cuprates with transition temperatures up to ~ 90 K [4–6]. Samples with similar doping levels show qualitatively a similar behavior. On lowering the temperature, underdoped cuprates display a suppression in the scattering rate below 700 cm^{-1}. This structure has been interpreted as

* Corresponding author. Fax: 352 392 0524; e-mail: axel.zibold@t-online.de, tanner@phys.ufl.edu.

0921-4526/98/$19.00
PII S0921-4526(97)00457-2

the opening of a pseudogap already well above T_c and is accompanied by the formation of a gap-like feature in the c-axis optical conductivity [7]. No indication of the pseudogap is reported for optimal and overdoped samples; optimally doped ones have the scattering rate suppression only below T_c whereas overdoped ones show no such indication at any temperature. In this paper we analyse the *ab*-plane optical properties of a $Tl_2Ba_2CaCu_2O_8$ (Tl2212) sample with $T_c = 110$ K. We discuss the far-infrared optical properties above and below T_c. Previous infrared measurement on single crystals have been reported for thin films and single crystals of $Tl_2Ba_2CaCu_2O_8$, with qualitatively similar results [8–10].

2. Experimental

Sample growth [10] and infrared techniques [11] have been described previously. We covered 130–40 000 cm^{-1} at 300 K and 130–4000 cm^{-1} at every temperature investigated (10, 35, 50, 90, 120, 160, 250, and 300 K). By 4000 cm^{-1}, temperature dependence was minimal. To obtain the complex optical conductivity or equivalently the dielectric function, we performed Kramers–Kronig analysis of the reflectance data. Extrapolations at low frequencies assumed either metallic or superconducting state, as appropriate. At high frequencies the room temperature reflectance was used followed by a weak power law and then by free-electron behavior [2, 3].

3. Results: reflectivity, conductivity, and scattering rate

Fig. 1 shows the far-infrared reflectance at four temperatures, two above and two below the superconducting transition temperature ($T_c = 110$ K). The reflectance increases as temperature is lowered; a significant shoulder develops at the lowest temperature. Below 600 cm^{-1} the spectra show sharp features, which can be attributed to as phonon modes. These features are considerably more prominent than in other cuprates [12]. The reflectance at 45° angle of incidence of the three-layer compound,

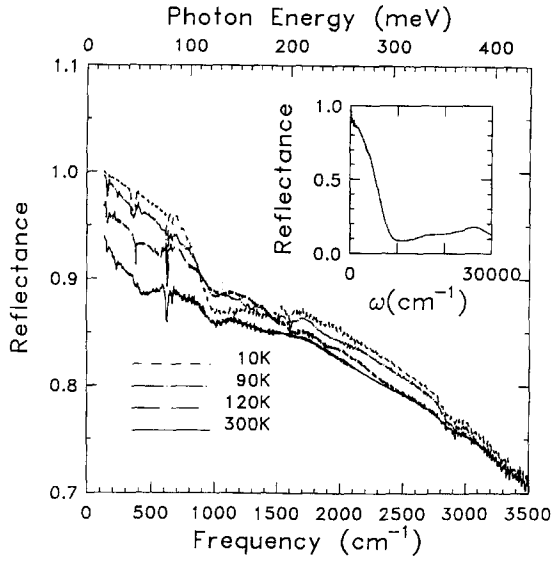

Fig. 1. Far-infrared reflectance of a $Tl_2Ba_2CaCu_2O_8$ sample ($T_c = 110$ K). The inset shows the room temperature spectrum on an extended scale.

$Tl_2Ba_2Ca_2Cu_3O_{10}$, shows strong longitudinal c-axis phonon modes. Because of the slight angle away from near-normal incidence in our unpolarized measurements, a similar explanation might hold for the observed modes [13]. For frequencies above about 3000 cm^{-1}, the spectra start to merge, implying most of the temperature dependence occurs for frequencies below this frequency. In the inset the room-temperature reflectance is shown up to 30 000 cm^{-1}. There is a plasmon minimum at 10 000 cm^{-1} and two electronic bands at 15 000 and 32 000 cm^{-1}.

The temperature evolution of the real part of the optical conductivity function $\sigma_1(\omega)$ over 175–2500 cm^{-1} is shown in the upper panel of Fig. 2. The normal-state conductivity is dominated at low temperatures by free-carrier-like behavior. Structures in the spectra can be seen from the phonon modes. For frequencies above about 2000 cm^{-1} the spectra begin to merge. Below T_c a significant amount of spectral weight is removed and transferred to the superconducting condensate delta function at zero frequency.

To describe the optical conductivity in a more general way we analyzed our data using a generalized

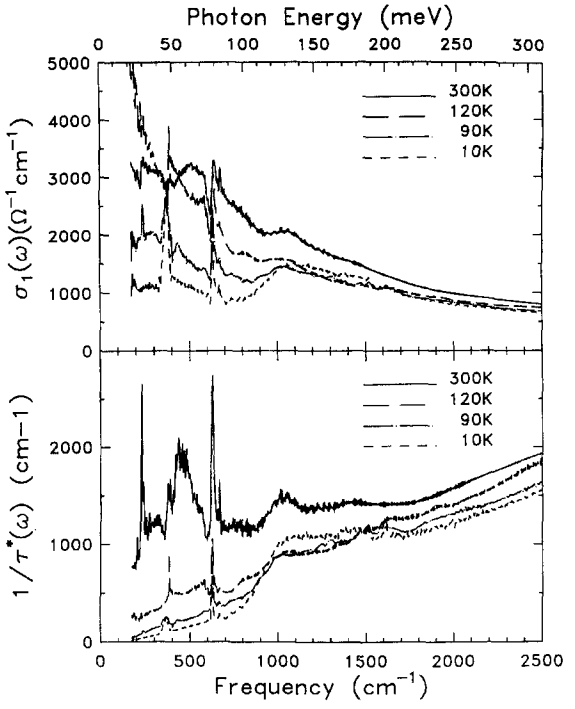

Fig. 2. Optical conductivity $\sigma_1(\omega)$ and scattering rate $1/\tau^*(\omega)$. In the superconducting state a depression can be clearly seen in $1/\tau^*$ below 1000 cm^{-1}.

Drude model [2, 3]. In this model, the frequency-dependent scattering rate can be obtained from the ratio of the Kramers–Kronig-determined imaginary to real parts $\sigma(\omega)$

$$\frac{1}{\tau^*(\omega)} = \frac{\omega\sigma_1(\omega)}{\sigma_2(\omega)}. \tag{1}$$

In the lower panel of Fig. 2 the scattering rate is plotted at four temperatures. The scattering rate shows some structures due to the phonons; however, the charge carrier response can be clearly seen.

The frequency-dependent scattering rate is clearly decreased on cooling from 300 to 120 K at all frequencies up to 2500 cm^{-1}. Below T_c there is a further decrease at high frequencies, but the behavior at these frequencies is dominated by a strong suppression below 1000 cm^{-1}. If we compare the data with results of various underdoped materials which are reported to be in the pseudogap state [5, 6], there is clearly different behavior. First, there is no obvious pseudogap behavior above T_c. Second, the temperature dependence at high temperatures is more consistent with optimally doped or even overdoped systems. However, the appearance of the suppression in the scattering rate below T_c is inconsistent with overdoped behavior. Thus, the overall temperature dependence of our data imply an optimal doping.

4. Penetration depth and carrier densities

A generalized penetration depth can be calculated below T_c from the imaginary part of the optical conductivity, $\sigma_2(\omega)$:

$$\lambda_L(\omega) = \frac{c}{\sqrt{4\pi\omega\sigma_2(\omega)}} = \frac{c}{\omega_{ps}(\omega)}, \tag{2}$$

with c the speed of the light and $\omega_{ps}(\omega)$ a generalized superfluid plasma frequency. $\lambda_L(\omega)$ is displayed for the lowest temperature in Fig. 3. It shows some structure due to the phonons; however, the plot is generally flat, demonstrating the London-like response in the superconducting state. The London penetration depth is the zero-frequency limit of $\lambda_L(\omega)$; we can estimate $\lambda_L = 1700$ Å. We can also estimate a superfluid density n_s from the plasma frequency $\omega_{ps} = 4\pi n_s e^2/m^*$, or, equivalently:

$$n_s = \frac{m^* c^2}{4\pi e^2}\frac{1}{\lambda_L^2}, \tag{3}$$

where m^* is the band electronic mass. We calculated this on a per copper basis, with 2 coppers/formula unit in $Tl_2Ba_2CaCu_2O_8$. Taking $m^* = m_e$, we found a value of $N_s = 0.115$ charge carriers per copper. The London penetration depth is also equal to

$$\lambda_L^2 = c^2/8 \int_0^\infty (\sigma_n(\omega) - \sigma_s(\omega))\, d\omega. \tag{4}$$

Evaluating Eq. (4) gave a similar number for the penetration depth.

Before making a comparison of the superfluid density to the carrier density, one must choose

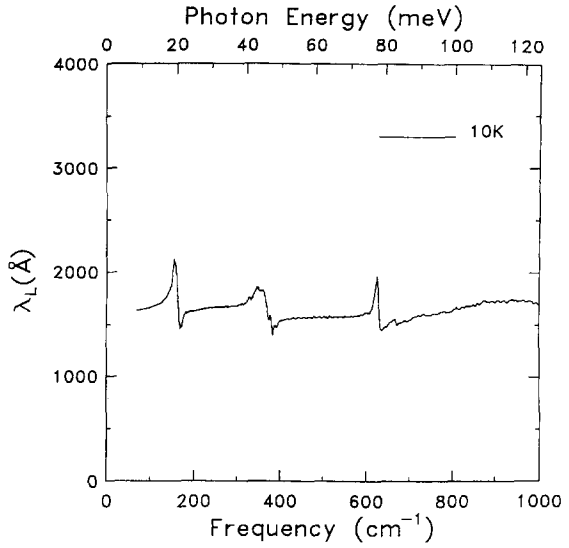

Fig. 3. The generalized London penetration depth of the 10 K spectrum.

whether to take a one-component or two-component perspective for the optical properties. In a one component picture, the comparison should be with the total spectral weight below the ~ 1.5 eV charge-transfer gap. The easiest way to obtain this is to use the conductivity sum rule. Here, the effective number of carriers per copper $N_{\mathrm{eff}}/N_{\mathrm{Cu}}$ can be found

$$N_{\mathrm{eff}} = \frac{2m_e V_{\mathrm{cell}}}{\pi e^2 N_{\mathrm{Cu}}} \int_0^{\omega_c} \sigma_1(\omega)\, \mathrm{d}\omega, \tag{5}$$

where V_{cell} is the unit cell volume and $N_{\mathrm{Cu}} = 2$. The cutoff frequency ω_c of the integration is chosen at the onset of the charge-transfer gap. We found an effective number of carriers $N_{\mathrm{eff}} = 0.54$ per copper. Within roughly 10% deviation this number can be also obtained from a Drude–Lorentz fit which uses a Drude term and Lorentz oscillators to describe the infrared conductivity. The effective number is given by the sum of the oscillator strengths of the Drude and those Lorentzian oscillators which have eigenfrequencies below ω_c.

In the two-component picture, the free carriers give rise to the the Drude term in the fit; the midinfrared carriers are assumed not to condense into the superfluid [2, 3]. This analysis gives a carrier number $N_D = 0.13$ per copper. Thus, about 20% of the total carrier density and about 90% of the free-carrier (Drude) density condenses into the delta function. These values have been shown to occur in most optimally doped cuprates [14]. See Table 1 for the results. Our $Tl_2Ba_2CaCu_2O_8$ sample has $T_c = 110$ K and, therefore, is expected to be very close to optimal doping.

5. Comparison to DC transport

To find the temperature evolution of the scattering rate of the Drude-type carriers in the two-component picture we fitted our reflectance (conductivity) data for each temperature using the Drude–Lorentz model. Above T_c this process is relatively straightforward. However, below T_c the procedure is complicated because part of the spectral weight of the free carriers moves into the condensate delta function at $\omega = 0$. Therefore, we used for the temperature-independent midinfrared contribution the 10 K conductivity data minus a small Drude term. (About 88% condenses; see Table 1.) We subtracted the midinfrared contribution from the higher-temperature data and obtained an estimate for the Drude contribution. Fig. 4 shows the scattering rate as a function of temperature. For comparison, the inset shows the DC resistivity of $Tl_2Ba_2CaCu_2O_8$. The DC resistivity is linear, and if the carrier density is constant,

Table 1
Effective number of carriers per copper in $Tl_2Ba_2CaCu_2O_8$

T_c (K)	N_{eff}	N_D	N_s	N_s/N_{eff}	N_s/N_D	λ_L (Å)
110	0.54	0.13	0.115	$21 \pm 1\%$	$88 \pm 4\%$	1700 ± 200

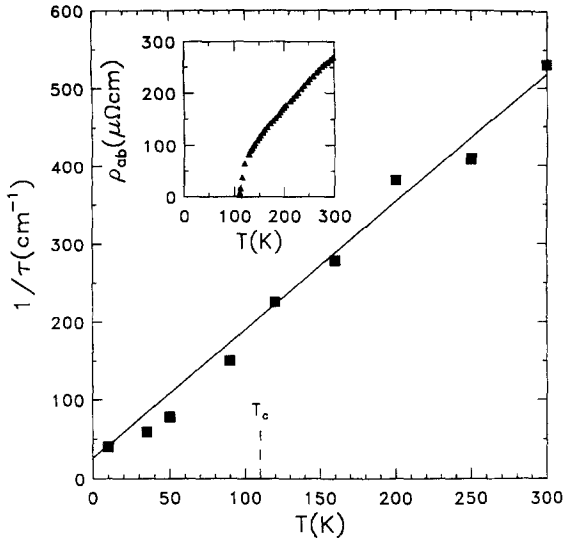

Fig. 4. Scattering rate as a function of temperature obtained by two-component analysis. The inset shows the *ab*-plane DC resistivity as a function of temperature.

$\rho_{ab} \sim 1/\tau_D$, consistent with the linear behavior from the optical measurements.

The temperature dependence of the scattering rate can be described in a simple model of electrons interacting with excitations. (In ordinary metals these excitations are the phonons. However, in the cuprates, they are almost certainly not ordinary phonons, but some other excitation, such as magnons, spin fluctuations, or other electrons.) In the high-temperature limit, one gets

$$1/\tau_D(T) = \lambda \frac{2\pi k_B}{\hbar} T + 1/\tau_0. \quad (6)$$

where λ is a dimensionless coupling constant representing the coupling of the free carriers to any kind of excitation process and τ_0 gives the elastic scattering rate, attributed to impurities. From a fit to the data above T_c, we obtain $1/\tau_0 = 26\,\mathrm{cm}^{-1}$ and $\lambda = 0.38$. This value of λ represents a weak coupling regime. The linear behavior of the scattering rate differs from the results of thermal-difference reflectance spectroscopy in $Tl_2Ba_2CaCu_2O_8$, where an optical scattering rate scaling as T^2 has been reported [15].

Below T_c only a portion N_q of the Drude carriers exists as quasiparticle excitations, because of condensation into the zero-frequency delta function of the superconductor. We take $N_q = N_D - N_s$ and estimate $1/\tau_D(T)$ below T_c using a Drude form for the quasiparticle conductivity. We find that we have a slight suppression of the scattering below T_c. There is no measurable change of slope above T_c; any decrease in $1/\tau_D(T)$ in the normal state could be interpreted as an indication for a pseudogap state. The scattering above, but close to, T_c yields $200\,\mathrm{cm}^{-1}$, a value smaller than the BCS gap, $2\Delta = 3.5\,k_B T_c = 268\,\mathrm{cm}^{-1}$. Thus, we can conclude that the material is in the clean limit.

6. Conclusions

The optical properties of $Tl_2Ba_2CaCu_2O_8$ differ from other cuprates in some ways but are similar in others. The similarities include the strong low-frequency but weak high-frequency temperature dependence, the absence of any sign of a superconducting gap in the data below T_c, and the linear scattering rate in the normal state far-infrared conductivity. Moreover, the fraction of the doping-induced spectral weight which condenses into the delta function (20%) is very close to the fraction condensed in other optimally-doped materials. The most striking difference is the strong phonon structure in the reflectance and conductivity, which may be due to the non-normal incidence in this very anisotropic material. Further work is underway to investigate this possibility. Also, the suppression of the quasiparticle damping below T_c is considerably smaller than in other materials. Finally, the scattering rate $1/\tau^*(\omega)$ does not show any sign of a pseudogap developing above T_c.

The magnitude of the scattering rate is smaller than the BCS gap, which puts the crystal in the clean limit. Finally, the overall behavior of $1/\tau^*(\omega)$ is consistent with optimal doping for this sample. The high value of T_c also suggests optimal doping.

Acknowledgements

This research has been supported by NSF Grant DMR–9403894.

References

[1] See the review article of B. Batlogg, Phys. Today 44 (1991) 44.
[2] T. Timusk, D.B. Tanner, in: D.M. Ginsberg (Ed.), Physical Properties of High Temperature Superconductors I, World Scientific, Singapore, 1989, p. 339.
[3] D.B. Tanner, T. Timusk, in: D.M. Ginsberg (Ed.), Physical Properties of High Temperature Superconductors III, World Scientific, Singapore, 1992, p. 363.
[4] D.N. Basov, R. Liang, B. Drabrowski, D.A. Bonn, W.N. Hardy, T. Timusk, Phys. Rev. Lett. 77 (1996) 4090.
[5] A.V. Puchkov, D.N. Basov, T. Timusk, J. Phys.: Condens. Matter 8 (1996) 10049.
[6] A.V. Puchkov, P. Fournier, D.N. Basov, T. Timusk, A. Kapitulnik, N.N. Kolesnikov, Phys. Rev. Lett. 77 (1996) 3212.
[7] C.C. Homes, T. Timusk, R. Liang, D.A. Bonn, W.N. Hardy, Phys. Rev. Lett. 71 (1993) 1645.
[8] C.M. Foster, K.F. Voss, T.W. Hagler, D. Milailovic, A.J. Heeger, M.M. Eddy, W.L. Olsen, E.J. Smith, Solid State Commun. 76 (1990) 651.
[9] G. Jehl, T. Zetterer, H.H. Otto, J. Schützmann, S. Shulga, K.F. Renk, Europhys. Lett. 17 (1992) 255.
[10] Allen M. Hermann, J.V. Yakhmi (Eds.), Thallium-Based High-Temperature Superconductors, Marcel Dekker, New York.
[11] F. Gao, D.B. Romero, D.B. Tanner, J. Talvacchio, M.G. Forrester, Phys. Rev. B 47 (1993) 1036.
[12] M.A. Quijada, D.B. Tanner, R.J. Kelley, M. Onellion, Z. Phys. B 94 (1994) 255.
[13] J.H. Kim, B.J. Feneestra, H.S. Somal, D. van der Marel, W.Y. Lee, A.M. Gerrits, A. Wittlin, Phys. Rev. B 49 (1994) 13065.
[14] D.B. Tanner, Y.-D. Yoon, A. Zibold, H.L. Liu, M.A. Quijada, S.W. Moore, J.M. Graybeal, O Beom-Hoan, J.T. Markert, R.J. Kelley, M. Onellion, J.-H. Cho, in: Ivan Bozovic, Dirk van der Marel (Eds.), Spectroscopic Studies of Superconductors, SPIE, Bellingham, Washington, 1996, pp. 13–23.
[15] M.J. Holcomb, C.L. Perry, J.P. Collman, W.A. Little, Phys. Rev. B 53 (1996) 6734.